Supplementary Information: Glucose deprivation activates a metabolic and signaling amplification loop leading to cell death

TABLE OF CONTENTS

SUPPLEMENTAL FIGURES

Supplemental Figure S1. Glucose withdrawal-induced death and supra-physiological phospho-tyrosine signaling do not require serum.

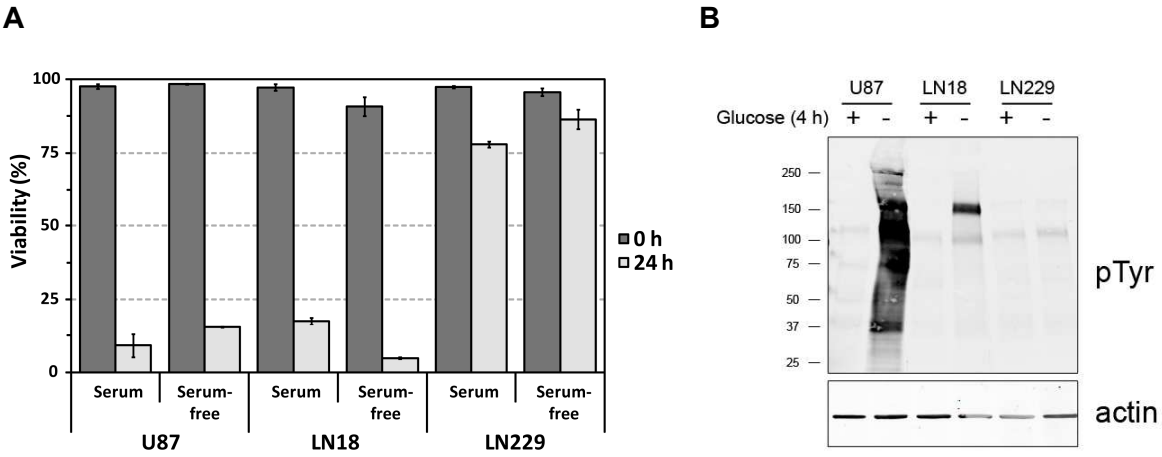

(**A**) GBM cell lines LN18, LN229 and U87 were starved of glucose for 24 h in the presence or absence of serum. Viability measurements by trypan blue exclusion revealed no significant differences between serum-stimulated and serum-starved cells following glucose withdrawal. (**B**) U87MG, LN18 and LN229 cells were serum-starved for 16 h and then starved of glucose and pyruvate for 4 h in the continued absence of serum. Western blotting revealed an induction of phospho-tyrosine signaling in the glucose withdrawal-sensitive cells (U87 and LN18) but not the glucose withdrawal-insensitive cells (LN229), consistent with results in serum-containing medium (Fig. 1A and B).

Supplemental Figure S2. Glutamine deprivation does not induce cell death or supra-physiological levels of tyrosine phosphorylation in U87-EGFRvIII cells.

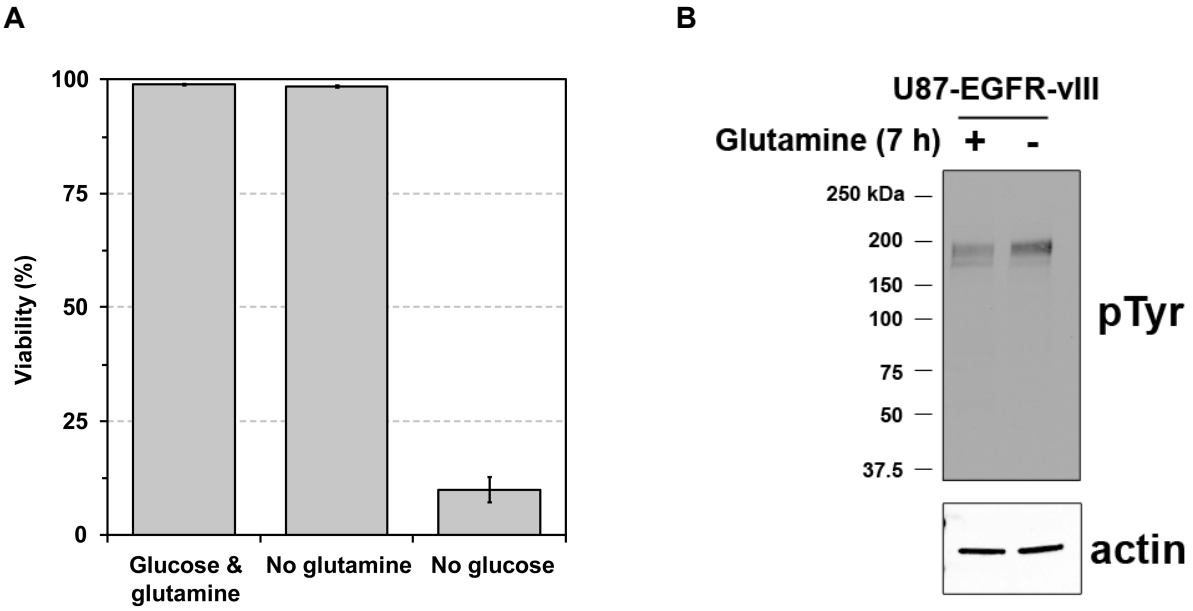

(**A**) U87-EGFRvIII cells were starved of either glucose or glutamine for 24 h, and viability was measured by trypan blue exclusion. Glucose, but not glutamine, starvation induced rapid and complete loss of cell viability. (**B**) Western blotting with an anti-phospho-tyrosine antibody demonstrated that glutamine-deprived U87-EGFRvIII cells do not show a dramatic upregulation of phospho-tyrosine signaling. Actin served as an equal loading control.

Supplemental Figure S3. Glucose withdrawal sensitivity of melanoma cell lines does not correlate with cell doubling time.

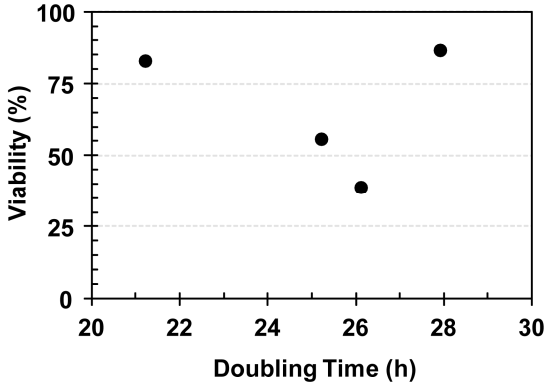

The sensitivity of four melanoma cell lines to glucose withdrawal does not correlate with cell doubling time (r = -0.19) (Nazarian *et al*, 2010).

Supplemental Figure S4. PTEN expression is reduced by genetic deletion and RNAi.

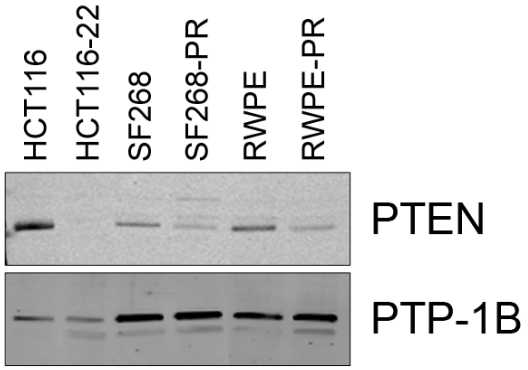

Western blotting demonstrated reduced PTEN expression in HCT116-22 (genetic deletion of *PTEN* by homologous recombination) and SF268-PR and RWPE-PR (shRNA-mediated RNAi), as compared to the respective parental controls. PTP-1B was used as an equal loading control. PR, PTEN-reduced.

Supplemental Figure S5. RNAi-mediated knockdown of PTEN in the glucose-withdrawal-sensitive cell line SF268 does not further increase glucose withdrawal sensitivity.

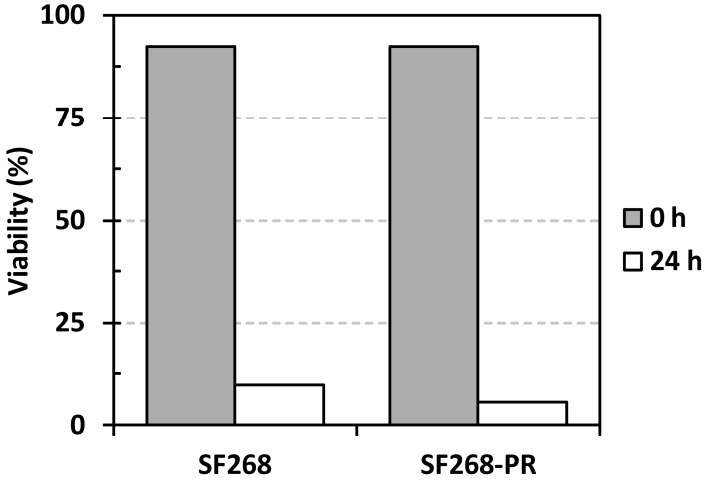

Expression of PTEN was reduced in SF268 GBM cells by shRNA-mediated RNAi, and cells were starved of glucose and pyruvate for 24 h. SF-269-PR cells showed similar levels of cell death following glucose withdrawal. PR, PTEN, reduced.

Supplemental Figure S6. Glucose withdrawal induces a signature of hyper-phosphorylation in U87-EGFRvIII that is associated with focal adhesions.

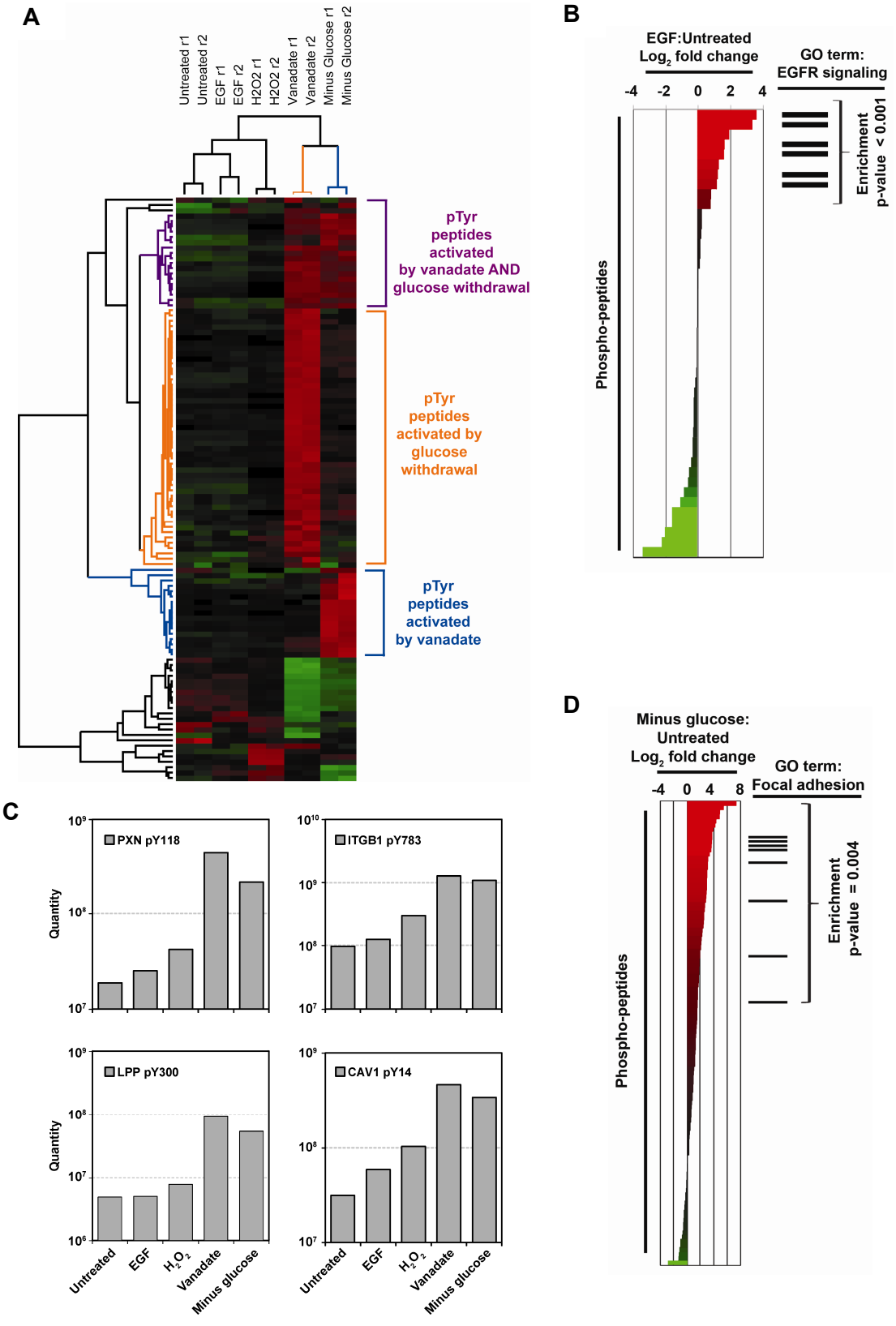

(**A**) Hierarchical clustering of tyrosine phosphorylation in U87-EGFRvIII cells reveals that glucose withdrawal induces a distinct set of phospho-events. U87-EGFRvIII cells were treated with four stimuli known to induce tyrosine phosphorylation, including a) EGF stimulation (10 ng/ml, 5 min), b) vanadate treatment (1 mM, 90 min), c) H_2O_2 (5 mM, 30 min) and d) glucose withdrawal (1.5 h). Changes in phospho-tyrosine signaling were measured by quantitative, label-free mass spectrometry (Rubbi *et al*, 2011) and data were hierarchically clustered. Each row of the heatmap depicts an individual phosphorylation event, and each column represents a sample as labeled. Samples were measured in technical duplicate (r1, r2). In the heatmap, red and green represent normalized levels of high and low phosphorylation, respectively. Branches of the dendrogram associated with upregulation by glucose withdrawal, upregulation by vanadate treatment, or upregulation by both are colored orange, blue and purple, respectively. (**B**) Phospho-events associated with the EGF signaling pathway are enriched in EGF-treated U87 cells. Phospho-peptides from U87 cells were ranked according to the measured $\log_2$ fold change in phospho-tyrosine levels following EGF stimulation and plotted on a waterfall plot, where the colors red and green represent increased or decreased tyrosine phosphorylation, respectively. Analysis of the phospho-peptides demonstrated an enrichment for proteins annotated with the GO term EGFR signaling pathway (GO:0007173) at the top of the ranked list (ie, increased phosphorylation following EGF stimulation) (permutation-based p-value < 0.001). Enrichment analysis of the phospho-peptides from EGF-treated U87-EGFRvIII cells revealed a similar enrichment (permutation-based p-value = 0.005, data not shown). (**C**) Glucose withdrawal induces increased phosphorylation in U87-EGFRvIII cells of proteins known to localize to focal adhesions. Phospho-tyrosine residues on paxillin (PXN Y118), integrin beta 1 (ITGB1 pY783), lipoma preferred partner (LPP pY300) and caveolin 1 (CAV1 pY14) show dramatically increased phosporylation in response to 1.5 h of glucose withdrawal. (**D**) Phospho-events associated with focal adhesions are enriched following glucose withdrawal in U87-EGFRvIII cells. Phospho-peptides from U87-EGFRvIII cells were ranked according to the measured $\log_2$ fold change in tyrosine levels following glucose withdrawal and plotted on a waterfall plot, where the colors red and green represent increased or decreased tyrosine phosphorylation, respectively. Analysis of the phospho-peptides demonstrated an enrichment for proteins annotated with the GO term Focal Adhesion (GO:0005925) at the top of the ranked list (ie, increased phosphorylation following glucose withdrawal) (permutation-based p-value = 0.004).

Supplemental Figure S7. Glucose withdrawal induces amplification of ROS in the glucose withdrawal-sensitive but not glucose withdrawal-insensitive cells.

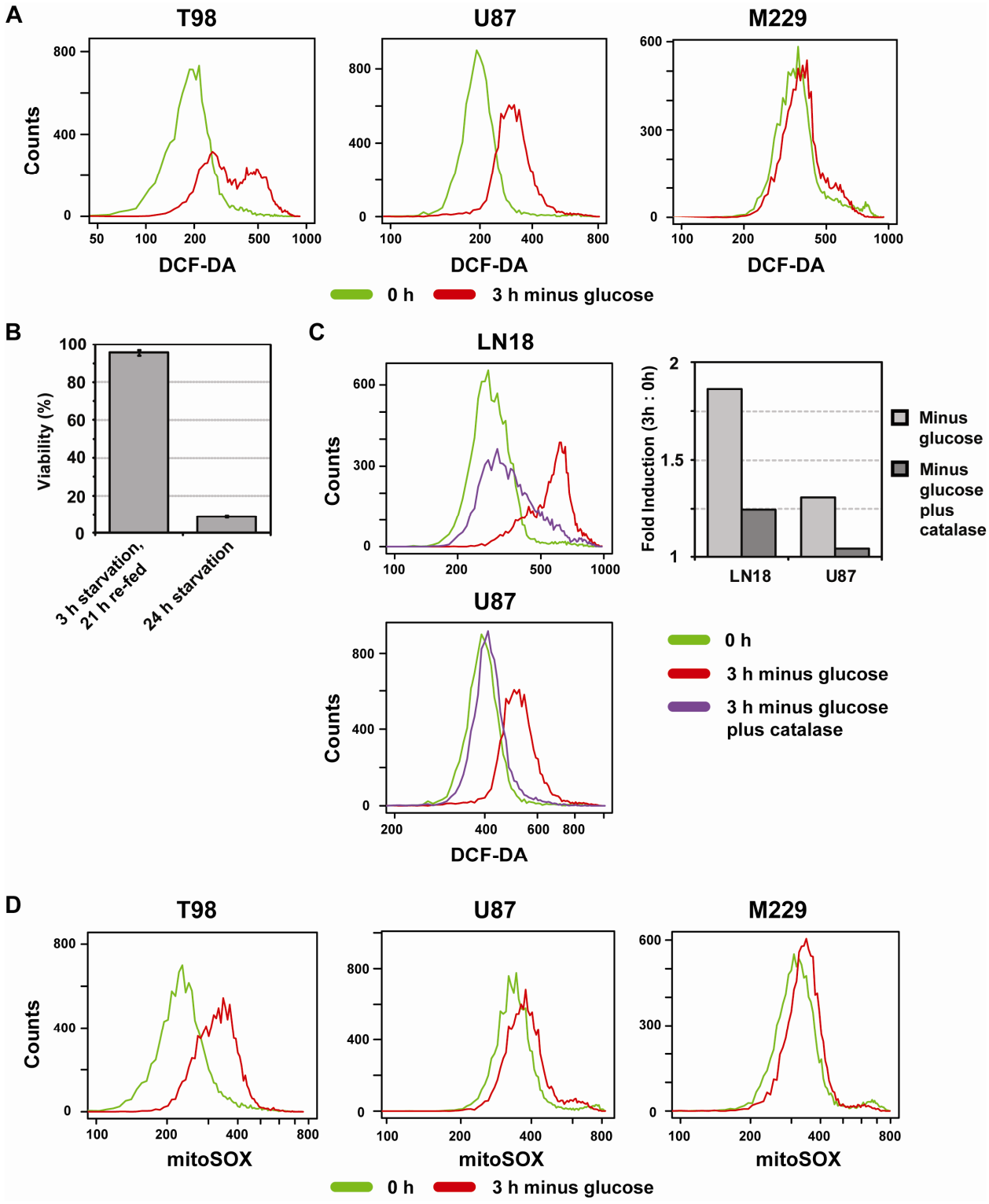

(**A**) T98, U87 and M229 cells were starved of glucose and pyruvate for 0 or 3 h, stained with the fluorescent ROS indicator DCF-DA (2.5 μM), and analyzed by flow cytometry. Histograms for T98 and U87 but not M229 show induction of ROS upon glucose withdrawal. (**B**) U87 cells are not committed to cell death after 3 h of glucose and pyruvate starvation. U87 cells starved of glucose and pyruvate for 3 h were either re-supplemented with glucose and pyruvate or left in starvation media for an additional 21 h. Viability was measured by trypan blue exclusion at 24 h. Error bars are the standard deviation of the mean (n = 3). (**C**) LN18 and U87 were starved of glucose and pyruvate with or without the H_2O_2 scavenger catalase (4 kU/ml) for 0 or 3 h. Glucose withdrawal-induced ROS was reduced in cells treated with catalase, as shown by both the histograms (left, center) and the reduction in the fold induction of mean fluorescent DCF-DA intensity (right). (**D**) Mitochondrial superoxide production is increased in glucose withdrawal-sensitive but not -insensitive cell lines. T98, U87 and M229 cells were starved of glucose and pyruvate for 0 or 3 h, stained with the mitochondrial superoxide probe mitoSOX (2.5 μM), and analyzed by flow cytometry.

Supplemental Figure S8. Glucose withdrawal-induced ROS mediate tyrosine kinase induction and cell death.

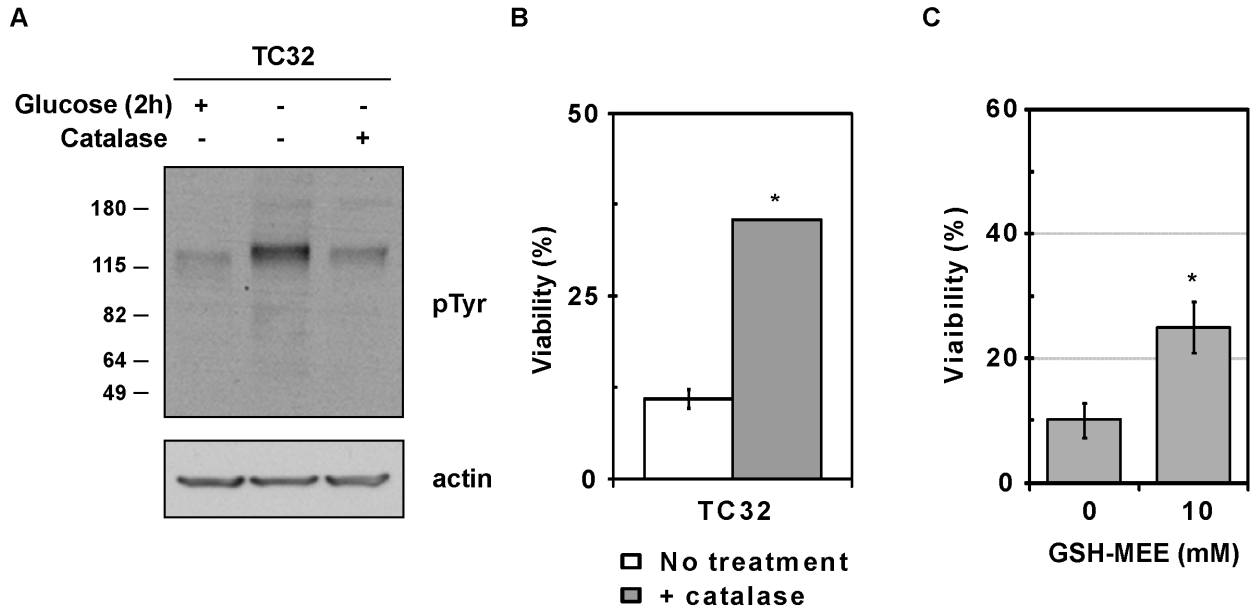

(**A**) The sarcoma cell line TC32 was starved of glucose and pyruvate for 2 h with or without the H_2O_2 scavenger catalase (1 kU/ml). Western blotting demonstrated that glucose withdrawal-induced phospho-tyrosine signaling requires catalase-sensitive ROS. Actin served as an equal loading control. (**B**) The sarcoma cell lines TC32 was starved of glucose and pyruvate with or without the H_2O_2 scavenger catalase, and viability was measured by trypan blue exclusion 24 h later. Catalase treatment rescued cells from glucose withdrawal-induced cell death ($p = 0.003$ (*) by Student's t-test, n = 3). (**C**) Reduced glutathione protects against glucose withdrawal-mediated cell death. U87-EGFRvIII cells were starved of glucose and pyruvate in the presence of the cell-permeable reduced glutathione (GSH-MEE) at the indicated concentrations. Viability was measured 24 h later by trypan blue exclusion ($p < 0.001$ (*) by Student's t-test). Error bars are standard deviation of the mean (n = 13 and 2 for 0 and 10 mM, respectively).

Supplemental Figure S9. siRNA-mediated knockdown of p22^{phox}.

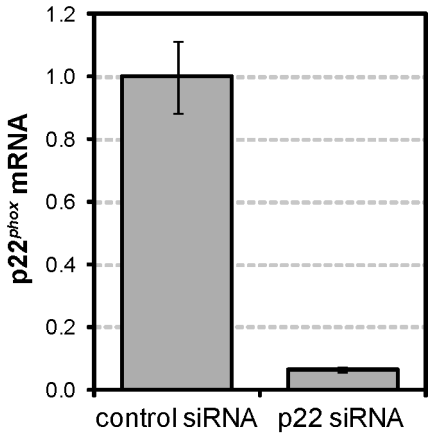

U87 cells were reverse transfected with 30 pM siRNA of either control, non-targeting siRNA or siRNA directed against p22^{phox}. Total RNA was isolated, reverse transcribed and used to quantify knockdown of p22^{phox} by qPCR. GAPDH was used as an internal normalization control. Error bars are the standard deviation of the mean (n = 3).

Supplemental Figure S10. Intracellular Ca2+ flux contributes to glucose withdrawal-induced mitochondrial superoxide production.

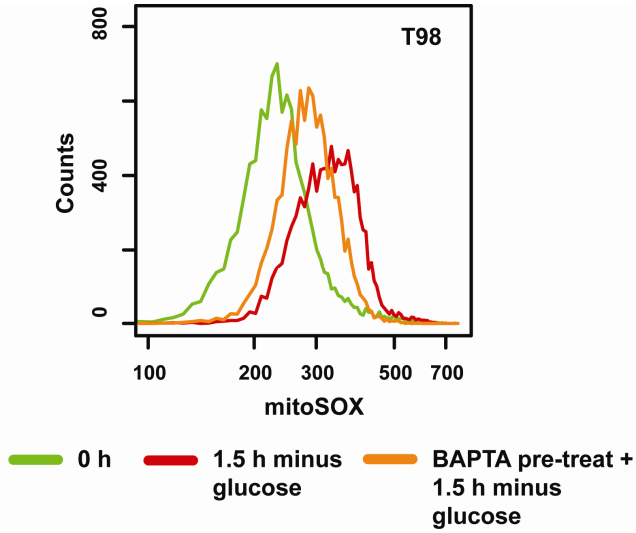

T98 cells were pre-treated for 1.5 h with 5 μM BAPTA-AM and then starved of glucose and pyruvate for 1.5 h before staining with mitoSOX and analysis by flow cytometry.

Supplemental Figure S11. Validation of ρ_0 cells.

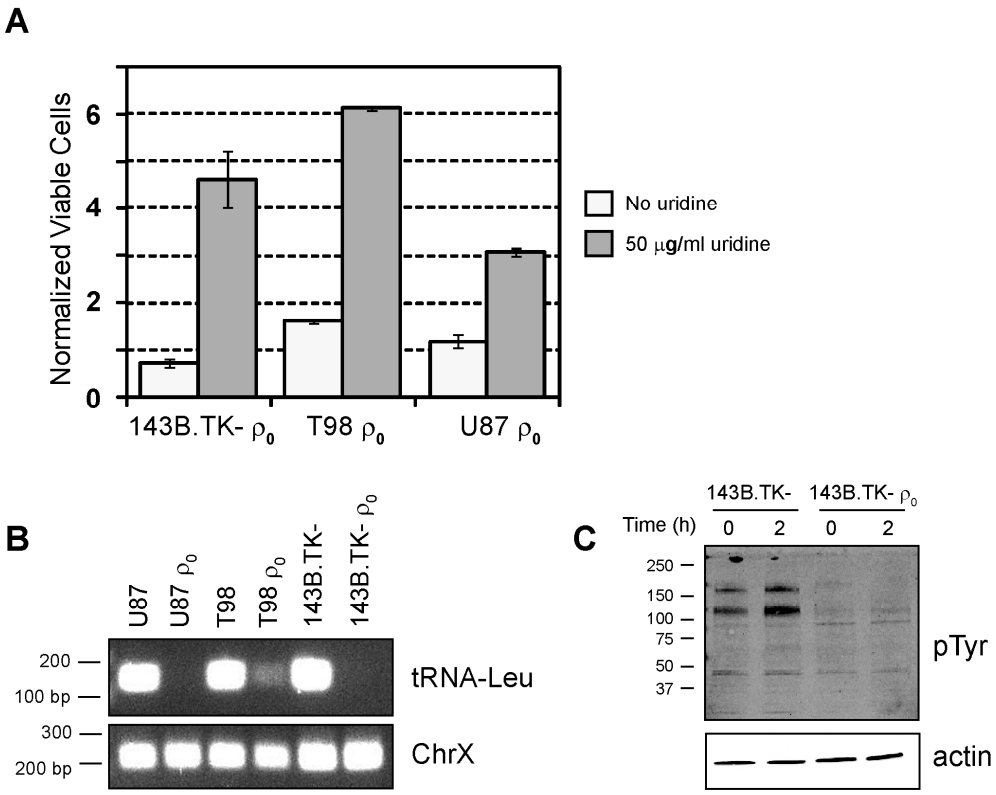

(**A**) ρ_0 cells are uridine auxotrophs. 143B.TK-, T98 and U87 ρ_0 cells were cultured with or without 50 μg/ml uridine for 3 days and the total number of viable cells was measured by trypan blue exclusion. (**B**) T98, U87 and 143B.TK- ρ_0 cells lack mitochondrial DNA. PCR against the mitochondrially-encoded tRNA-Leu was performed to assess the presence or absence of the mitochondrial genome. PCR against a portion of the nuclear X chromosome was included as a loading control. (**C**) Mitochondrial ROS production is required for glucose withdrawal-induced phospho-tyrosine signaling. Parental and ρ_0 143B.TK- cells were starved of glucose and pyruvate for the indicated times. Western blotting with an anti-phospho-tyrosine antibody demonstrated that parental but not ρ_0 cells exhibit upregulation of phospho-tyrosine signaling after glucose withdrawal. Actin served as an equal loading control.

Supplemental Figure S12. Glucose withdrawal-induced ROS mediate oxidative inhibition of protein tyrosine phosphatases.

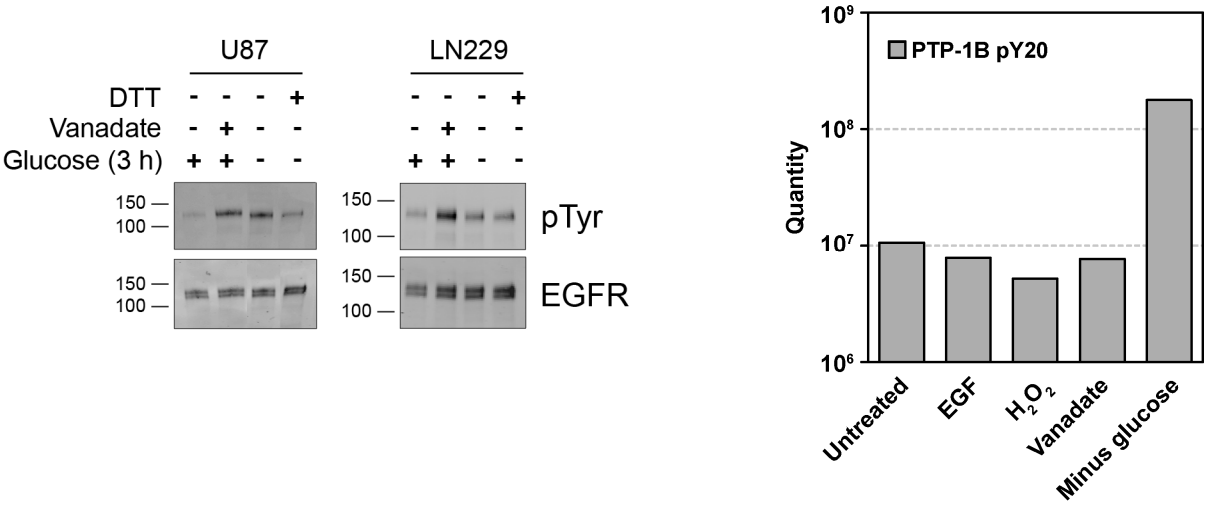

(**A**) Glucose withdrawal causes oxidative inhibition of PTP activity in glucose withdrawal-sensitive but not in insensitive cell lines. U87 and LN229 cells were starved of glucose for 0 or 3 h, and the ability of cell lysates to dephosphorylate EGFRvIII was measured by quantitative Western blotting. Vanadate (1 mM) and DTT (2 mM) were added to the dephosphorylation reaction as a negative control and a reducing agent, respectively. Relative phosphatase activity was normalized to the vanadate control. A representative blot is shown. (**B**) Glucose withdrawal upregulates phosphorylation of PTP-1B. Quantitative, label-free mass spectrometry revealed that Y20 of PTP-1B was specifically upregulated in U87 cells starved of glucose and pyruvate for 3 h.

Supplemental Figure S13. Phosphatase inhibition induces ROS.

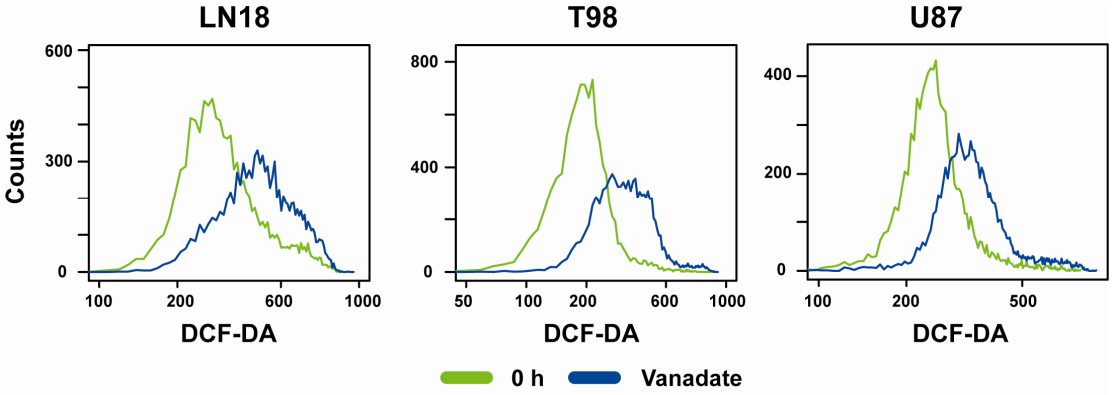

LN18, T98 or U87 cells were treated with the PTP inhibitor vanadate (200 mM) for 3 h, stained with oxidation-sensitive fluorogen DCF-DA and analyzed by flow cytometry. Histogram plots demonstrate that vanadate increases DCF-DA in all cell lines tested.

REFERENCES

Nazarian R, Shi HB, Wang Q, Kong XJ, Koya RC, Lee H, Chen ZG, Lee MK, Attar N, Sazegar H, Chodon T, Nelson SF, McArthur G, Sosman JA, Ribas A, Lo RS (2010) Melanomas acquire resistance toB-RAF(V600E) inhibition by RTK or N-RAS upregulation. *Nature* **468:** 973-U377.

Rubbi L, Titz B, Brown L, Galvan E, Komisopoulou E, Chen SS, Low T, Tahmasian M, Skaggs B, Muschen M, Pellegrini M, Graeber TG (2011) Global phosphoproteomics reveals crosstalk between Bcr-Abl and negative feedback mechanisms controlling Src signaling. *Sci Signal* **4:** ra18.